MATHEMATICS OF COMPUTATION
Volume 70, Number 235, Pages 1071–1088
S 0025-5718(00)01237-0
Article electronically published on November 27, 2000

NUMERICAL TESTING OF THE STABILITY OF VISCOUS SHOCK WAVES

LEON Q. BRIN

ABSTRACT. A new theoretical Evans function condition is used as the basis of a numerical test of viscous shock wave stability. Accuracy of the method is demonstrated through comparison against exact solutions, a convergence study, and evaluation of approximate error equations. Robustness is demonstrated by applying the method to waves for which no current analytic results apply (highly nonlinear waves from the cubic model and strong shocks from gas dynamics). An interesting aspect of the analysis is the need to incorporate features from the analytic Evans function theory for purposes of numerical stability. For example, we find it necessary, for numerical accuracy, to solve ODEs on the space of wedge products.

1. INTRODUCTION

Stability is an important issue for any evolutionary system. It is the arbiter in questions of possible asymptotic states and physically attainable solutions. The problem of stability of viscous shock waves dates back to treatment of the scalar case in the late 1950's [20]. Despite the efforts of many since then, no analytic results exist which determine the stability of strongly nonlinear viscous shocks. However, a theoretical stability criterion (necessary and sufficient condition) has been developed by Zumbrun and Howard [22] in terms of the Evans function. The Evans function is an analytic function introduced by Evans [5, 6, 7, 8] for the purpose of locating eigenvalues of nonnormal ordinary differential operators, and developed into its present form by Alexander, Gardner and Jones [1]. The objective of this paper is to develop a flexible computer program which evaluates the criterion in a way that is suitable for rapid determination of stability of *all* types of viscous shock waves.

The present work is related to that done by Daniel Michelson [18, 19]. He carried out a numerically assisted proof of the stability of the Bunsen flame profiles in the Kuramoto-Sivashinsky equations. However, there are some differences between his work and the present work. Michelson dealt with an operator with no kernel, and he used an interior method. That is, he performed a numerical calculation on a grid of points covering a region of the complex plane. In this work, we will deal with an operator with kernel, and use a method requiring calculations only on a grid along the boundary of a region of the complex plane.

Received by the editor January 4, 1999 and, in revised form, June 24, 1999.
2000 *Mathematics Subject Classification.* Primary 35B35, 65L70, 35-04; Secondary 35L65.

In addition to Michelson's work, several other developments in Evans function theory were critical to the development of the present algorithm. Alexander, Gardner and Jones [1] proved the analyticity of the Evans function away from the essential spectrum, in particular in the right complex half plane. More recently, Gardner and Zumbrun [10] and Kapitula and Sandstede [13] independently proved that the Evans function can be analytically extended part way into the essential spectrum, thus the left complex half plane. A version of this result is presented in Theorem 1. This result, paired with Zumbrun and Howard's necessary and sufficient condition for stability, leads to our numerical algorithm for determining linear stability of viscous shocks.

As in the work of Michelson [18], the problem is first reduced to counting the zeroes of the Evans function in a bounded region. In contrast to [18], a winding number argument is then used to count the zeroes. Some issues that arise and are resolved include the following.

First, the second fastest growing mode of a particular ODE cannot be computed individually since the fastest growing mode dominates the numerical solution. This is a type of stiffness which is handled by doing the computation in wedge space (see subsection 3.3).

Second, inherent in the computation of the Evans function is the possibility that numbers of nearly equal magnitude will be subtracted, resulting in a large loss of significance: loss of 4 significant digits has been encountered. This leads to the need for sharp error estimates. Linearity of the eigenvalue equation and of the Runge-Kutta method are exploited to derive a posteriori error estimates which approximate the actual error within a few orders of magnitude (see subsection 3.4).

Third, the Evans function must be evaluated at sufficiently many points on the boundary of the bounded region that the reported winding number is correct. An adaptive stepping algorithm based on the values of the Evans function and its derivatives is developed for this purpose (see subsection 3.3).

In Section 4, application of the algorithm to several test cases will demonstrate accurate evaluation of the Evans function (and therefore accurate prediction of stability or instability), plus stability of viscous shock waves to which no current analytic results apply.

2. Preliminaries

2.1. **Basic definitions.**

Definition 1 (Viscous shock wave)**.** A viscous shock wave is a traveling wave solution, $\overline{u}$, of the n-component conservation law

$$u_t + (f(u))_x = (B(u)u_x)_x \tag{1}$$

such that $\overline{u}'(\pm\infty) = 0$, $\overline{u}(\pm\infty) = \overline{u}_\pm$.

Such waves are found by using the ansatz $u(x,t) = \overline{u}(x - st)$ (a traveling wave where s is the speed of propagation) in equation (1). Integrating from $-\infty$ to x and enforcing the boundary conditions gives the traveling wave ODE

$$-s(\overline{u} - \overline{u}_-) + f(\overline{u}) - f(\overline{u}_-) = B(\overline{u})\overline{u}'. \tag{2}$$

Any solution to this equation with appropriate behavior at $\pm\infty$ is a viscous shock wave for equation (1). Having fixed $\overline{u}_-$ and s, the Rankine-Hugoniot condition

$$-s(\overline{u}_+ - \overline{u}_-) + f(\overline{u}_+) - f(\overline{u}_-) = 0 \tag{3}$$

is used to solve for the possible values of $\overline{u}_+ = \overline{u}(\infty)$.

Definition 2 (Viscous shock wave manifold)**.**

$$M = \{\overline{u}_\delta : \overline{u}_\delta \text{ is a viscous shock wave solution of (1)}, \delta \in U \subseteq \mathbb{R}^\ell, U \text{ open}\}$$

is called the viscous shock wave manifold for (1) if δ continuously indexes all viscous shock wave solutions of (1) with fixed end states, $\overline{u}_\pm$.

Definition 3 (Orbital stability)**.** A viscous shock wave $\overline{u}$ is called orbitally stable if, for each solution u of (1) with $|u(x,0) - \overline{u}(x)|$ sufficiently small, there exists $\delta(u) \in \mathbb{R}^\ell$ such that $\overline{u}_\delta \in M$ and

$$u \to \overline{u}_\delta \quad \text{as} \quad t \to \infty.$$

Exactly how small $|u(x,0) - \overline{u}(x)|$ should be is still under investigation. Current results [22] require $|u(x,0) - \overline{u}(x)| \leq \epsilon(1 + |x|)^{-r}$ for some $r \geq 3/2$.

2.2. **The Evans function.** The linear evolution operator associated with equation (1) is obtained by making the change of variables $\tau = t$, $\xi = x - st$, and linearizing about the resulting stationary viscous shock wave solution. The result is $w_\tau = Lw$, where

$$Lw = -(A(\xi)w)_\xi + (B(\xi)w_\xi)_\xi \tag{4}$$

and A is defined by

$$A(\xi)w = f'(\overline{u}(\xi))w - sw - B'(\overline{u}(\xi))w\overline{u}'(\xi). \tag{5}$$

Stability is related to the spectrum of L, but not in a direct way, since the essential spectrum accumulates at the origin [22]. The precise relation comes from analysis of the Evans function.

To define the Evans function, rewrite the eigenvalue equation, $Lw = \lambda w$, using (4) to get

$$(B(\xi)w')' = (A(\xi)w)' + \lambda w \qquad w(\pm\infty) = 0,\ w'(\pm\infty) = 0, \tag{6}$$

where a prime denotes a derivative with respect to ξ. Now let $W = \binom{w}{w'}$ and express (6) as the first order system

$$W' = \tilde{A}(\xi)W, \qquad W(\pm\infty) = 0, \tag{7}$$

where

$$\tilde{A}(\xi) = \begin{pmatrix} 0 & I \\ B^{-1}(\xi)(\lambda I + A'(\xi)) & B^{-1}(\xi)(A(\xi) - B'(\xi)) \end{pmatrix}. \tag{8}$$

Further, let $Y^- \equiv \{W_1^-(\xi), \ldots, W_{n^-}^-(\xi)\}$ be a basis for the solutions W which decay to 0 as $\xi \to -\infty$, and let $Y^+ \equiv \{W_1^+(\xi), \ldots, W_{n^+}^+(\xi)\}$ be a basis for the

solutions W which decay to 0 as $\xi \to \infty$. If $n^- + n^+ = 2n$, then the Evans function is defined by

$$D(\lambda) = \det \begin{pmatrix} W_1^+(0) \\ \vdots \\ W_{n^+}^+(0) \\ W_1^-(0) \\ \vdots \\ W_{n^-}^-(0) \end{pmatrix}.$$

Notice that $D(\lambda) = 0$ implies linear dependence of the vectors in $Y^- \cup Y^+$. Since Y^- and Y^+ are (individually) linear independent sets, linear dependence of the vectors in $Y^- \cup Y^+$ implies the existence of a vector, W_0 (determined by some linear combination of the $W_i^+(0)$ or $W_i^-(0)$), such that the solution of (7) with initial conditions $W(0) = W_0$ decays in both forward and backward time. In other words, λ is an eigenvalue of L.

Now, since $\overline{u}$ approaches constant values at plus and minus infinity, $\tilde{A}$ also approaches constant values, $\tilde{A}^\pm$, at plus and minus infinity. In fact, $\lim_{\xi\to\infty} |\tilde{A}^+ - \tilde{A}(\xi)| = O(e^{\alpha^+\xi})$ for some $\alpha^+ < 0$, and $\lim_{\xi\to-\infty} |\tilde{A}^- - \tilde{A}(\xi)| = O(e^{\alpha^-\xi})$ for some $\alpha^- > 0$. So, for each negative eigenvalue μ_i^+ of $\tilde{A}^+$ and positive eigenvalue μ_i^- of $\tilde{A}^-$, the asymptotic estimate (similar to one in [4])

$$W_i^\pm(\xi) = \left(1 + O(e^{\alpha^\pm\xi})\right) e^{\mu_i^\pm \xi} V_i^\pm, \qquad i = 1, 2, \ldots, n^\pm, \tag{9}$$

can be used to approximate $W_i^\pm(\xi_0^\pm)$ for some large $|\xi_0^\pm|$ (see Theorem 1 below). In essence, estimates (9) solve equation (7) on the complement of (ξ_0^-, ξ_0^+). These values can then be used as "initial" conditions in solving equation (7) for the needed quantities $W_i^\pm(0)$.

However, using equation (9) assumes knowledge of $\mu_i^\pm$ and $V_i^\pm$, the eigenvalues and eigenvectors of $\tilde{A}^\pm$, which generally will be obtained numerically. But, when the eigenvalues and eigenvectors of $A^\pm$ are known and $B = I$, determining μ_i and V_i is trivial [2]. Also, when $B = I$ and $\mathrm{Re}(\lambda) > 0$, $\tilde{A}^\pm$ has n positive and n negative eigenvalues [2], implying $n^- + n^+ = 2n$, and the Evans function is well defined in the right half plane.

2.3. **The Gap Lemma.** A critical tool in the development of our algorithm is the Gap Lemma. As applied in the context of the previous section, it provides a means for computing the $W_i^\pm(0)$ necessary for evaluation of the Evans function. Just as importantly, it supplies a condition for establishing the analyticity of the $W_i^\pm(0)$ (and therefore the Evans function) as functions of λ. A definition and a standard lemma of matrix theory [14] are necessary to elucidate its statement.

Definition 4 (Spectral gap)**.** Let A be a matrix and μ one of its eigenvalues. Then the spectral gap g is given by

$$g(\mu) = \mathrm{Re}(\mu) - \max\{\mathrm{Re}(\xi) : \xi \in \sigma(A), \xi \neq \mu\}.$$

Lemma 1. *Let A be a matrix and $\gamma = \max\{\mathrm{Re}(\xi) : \xi \in \sigma(A)\}$. Then, for any $\tilde{\gamma} > \gamma$, there exists $C(\gamma)$ so that*

$$|e^{At}| \leq C(\tilde{\gamma}) e^{\tilde{\gamma} t}.$$

Theorem 1 (The Gap Lemma). *Let $A(x,\lambda)$ be a matrix such that there exist constants $M > 0$, $C_1 > 0$, and $\alpha > 0$ so that $|A(y,\lambda) - A(-\infty,\lambda)| \le C_1 e^{\alpha y}$ for all $y \le -M$. If $\mu(\lambda)$ is an eigenvalue of $A(-\infty,\lambda)$ with associated eigenvector $V(\lambda)$ such that*

(i) *$A(-\infty,\lambda), \mu, V$ are analytic in λ in a neighborhood of λ_0,*
(ii) *$g(\mu) > -\alpha$ at λ_0, and*
(iii) *M is so large that $C_1 C_2 e^{-M\alpha}/(\tilde{\gamma}+\alpha) < 1/2$ where $\tilde{\gamma}$ and C_2 are the constants guaranteed by Lemma 1,*

then there exists a solution $\varphi(x,\lambda)$ of $W' = AW$ with

$$|\varphi(x,\lambda) - e^{\mu(\lambda)x}V(\lambda)| \le \frac{2C_1C_2e^{\alpha x}}{\tilde{\gamma}+\alpha}|e^{\mu(\lambda)x}V(\lambda)| \tag{10}$$

for all $x \le -M$. Further, φ is analytic in λ in a neighborhood of λ_0.

This is a special case of the Gap Lemma proved in [10, 13] with error bounds explicitly stated for numerical use. The Gap Lemma extends standard results (e.g., [4]) to the case of negative spectral gap. See [2] for proof. The analogous statement for A^+ holds as well of course.

2.4. **Stability criterion.** The main driving force for the algorithm of this paper is the following theorem [22].

Theorem 2 (Stability criterion). *A necessary and sufficient condition for linear orbital stability of viscous shock waves is that the number of zeroes of the Evans function in $\{\mathrm{Re}(\lambda) \ge 0\}$ equals the dimension ℓ of the viscous shock wave manifold M.*

This result reduces the question of stability to counting zeroes of the *analytic* Evans function.

3. The algorithm

3.1. **Overview.** Theorem 2 suggests the following algorithm.

1. Find a bounded region, $\Omega \subset \mathbb{C}$, which contains all the zeroes of D in the closed right half plane.
2. Apply the argument principle [21] to Ω to find the number of zeroes of D in the closed right half plane.
3. The viscous shock wave is stable *if and only if* the number from 2 equals the dimension of the viscous shock wave manifold.

3.2. **Bounding the search.** By an energy estimate [2] on equation (6), the zeroes of the Evans function must lie in the truncated wedge

$$V = \{\lambda \in \mathbb{C} : \mathrm{Im}(\lambda) + \mathrm{Re}(\lambda) \le r,\ \mathrm{Im}(\lambda) - \mathrm{Re}(\lambda) \ge -r,\ \mathrm{Re}(\lambda) \le r/4\},$$

where $r = \|f(\xi)\|_\infty^2/\|B\|_2$, $f(\xi) = \|A(\xi)\|_2$ (see Figure 1). Obviously, this is not a bounded region, though. By Theorem 2, the search may be limited to the portion of the wedge intersecting the closed complex right half plane, so we take $\Omega = V \cap \{\lambda \in \mathbb{C} : \mathrm{Re}(\lambda) \ge 0\}$. Also, we define $\Gamma \doteq \partial\Omega$.

Since the argument principle will be used to count the zeroes inside Ω, care must be taken that Γ does not contain any of the zeroes. However, $D(0) = 0$ with multiplicity at least the dimension of the viscous shock wave manifold [12], so the argument principle may not be applied to any region whose boundary includes

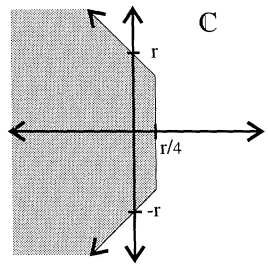

FIGURE 1. Stability is reduced to counting zeroes of the Evans function in a truncated wedge.

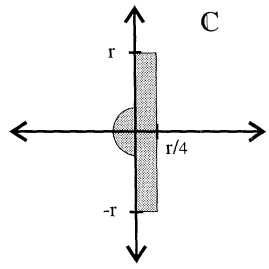

FIGURE 2. Modification of Ω to accommodate the origin, where $D = 0$.

the origin. Luckily, the Gap Lemma indicates a domain of analyticity including a neighborhood of the origin. So it is allowable to modify Ω slightly to accommodate the origin. A natural choice is to extend Ω in a semicircular fashion around the origin, and for simplicity force the straight line boundary segments of Ω parallel to the axes (see Figure 2). Of course, there is a limit, depending on α, to the size of the semicircle. For example, its radius is usually limited by the branchpoints of $\mu_i^{\pm}$ when $n = 2$.

Taking Ω as in Figure 2 leads to counting the zeroes of D in the right half plane, at the origin, plus, potentially, some in the left half plane. So when the computed winding number exceeds the dimension of the viscous shock wave manifold, the "extra" eigenvalues must be located at least approximately. If they have negative real parts (i.e., they lie in the semicircle), then the wave being tested is stable; otherwise, the wave is unstable. The occurence of an "extra" eigenvalue arises in testing viscous shock waves for the cubic model, for example (see subsection 4.2).

3.3. **Applying the argument principle.** The first problem in calculating the winding number of $D[\Gamma]$ lies in evaluating $D(\lambda)$ for a fixed value λ. This appears to be easy. As described in subsection 2.2, equation (7) must be solved for $W(0)$ once for each of $2n$ different "initial" conditions. A naive approach might be to do this directly, solving equation (7) $2n$ times. However, the numerical solution of (7) is dominated by the fastest growing mode. So, regardless of the initial conditions $W(\xi_0)$, $|\xi_0|$ large enough, the numerical solution for $W(0)$ will be a scalar multiple of the fastest growing mode, which of course is incorrect. A second attempt might be to solve for all of the modes simultaneously, subtracting from the slower growing modes their components in the direction of the faster growing modes at each step.

However, in practice this is equally unsuccessful in producing the correct values for the slower modes at 0.

It turns out that solving for the modes simultaneously is a good idea, but orthogonalization is not how to do it. Instead, the wedge product should be used. The wedge product as used here is strictly a bookkeeping tool. No reference to differential forms is made or implied. Instead, we consider the operator $\wedge$ defined on the standard basis vectors of $\mathbb{C}^m$ by the properties

$$\begin{aligned} &e_i \wedge (e_j + xe_k) = e_i \wedge e_j + xe_i \wedge e_k, \\ &(e_i + xe_j) \wedge e_k = e_i \wedge e_k + xe_j \wedge e_k \qquad \text{(bilinearity)}, \end{aligned}$$

and

$$e_i \wedge e_j = -e_j \wedge e_i \qquad \text{(antisymmetry)}.$$

This definition extends to an operation

$$\wedge : \mathbb{C}^{\binom{m}{i}} \times \mathbb{C}^{\binom{m}{j}} \longrightarrow \mathbb{C}^{\binom{m}{i+j}} \tag{11}$$

by writing each vector as a linear combination of its basis vectors. A vector $v \in \mathbb{C}^{\binom{m}{i}}$ in this context is referred to as an i-form. For example, if $m = 4$ and $x, y \in \mathbb{C}^{\binom{m}{1}}$ (i.e., x and y are 1-forms), then the 2-form $x \wedge y$ is computed as follows:

$$\begin{aligned} x \wedge y &= \begin{pmatrix} x_1 \\ x_2 \\ x_3 \\ x_4 \end{pmatrix} \wedge \begin{pmatrix} y_1 \\ y_2 \\ y_3 \\ y_4 \end{pmatrix} = \left(\sum_{i=1}^{4} x_i e_i \right) \wedge \left(\sum_{j=1}^{4} y_j e_j \right) \\ &= \sum_{i=1}^{4} \sum_{j=1}^{4} x_i e_i \wedge y_j e_j = \sum_{i=1}^{4} \sum_{j=1}^{4} x_i y_i e_i \wedge e_j \\ &= \sum_{i=1}^{3} \sum_{j=i+1}^{4} (x_i y_j - x_j y_i) e_i \wedge e_j = \begin{pmatrix} x_1 y_2 - x_2 y_1 \\ x_1 y_3 - x_3 y_1 \\ x_1 y_4 - x_4 y_1 \\ x_2 y_3 - x_3 y_2 \\ x_2 y_4 - x_4 y_2 \\ x_3 y_4 - x_4 y_3 \end{pmatrix}. \end{aligned} \tag{12}$$

It follows that the Evans function,

$$D(\lambda) = \det \begin{pmatrix} W_1^+(0) \\ \vdots \\ W_{n^+}^+(0) \\ W_1^-(0) \\ \vdots \\ W_{n^-}^-(0) \end{pmatrix} \tag{13}$$

can also be written as

$$D(\lambda) = W_1^+(0) \wedge \cdots \wedge W_{n^+}^+(0) \wedge W_1^-(0) \wedge \cdots \wedge W_{n^-}^-(0) \tag{14}$$

where, again, the wedge product is to be interpreted as an element of $\mathbb{C}^{\binom{2n}{2n}} = \mathbb{C}$.

Using the notation

$$\mathcal{W}^{\pm} = W_1 \wedge \cdots \wedge W_{n^{\pm}},$$

the Evans function is expressed as

$$D(\lambda) = \mathcal{W}^{+} \wedge \mathcal{W}^{-}.$$

Moreover, since each $W_i^{\pm}$ satisfies the linear ODE $W' = \tilde{A}W$, $\mathcal{W}^{\pm}$ satisfies the *linear* ODE

$$\begin{aligned}(\mathcal{W}^{\pm})' &= \sum_{i=1}^{n^{\pm}} W_1^{\pm} \wedge \cdots \wedge W_{i-1}^{\pm} \wedge (W_i^{\pm})' \wedge W_{i+1}^{\pm} \wedge \cdots \wedge W_{n^{\pm}}^{\pm} \\ &= \sum_{i=1}^{n^{\pm}} W_1^{\pm} \wedge \cdots \wedge W_{i-1}^{\pm} \wedge \tilde{A}W_i^{\pm} \wedge W_{i+1}^{\pm} \wedge \cdots \wedge W_{n^{\pm}}^{\pm}. \end{aligned} \tag{15}$$

Relationships (15) then define matrices $\mathcal{A}^{\pm}$ such that

$$(\mathcal{W}^{\pm})' = \mathcal{A}^{\pm}\mathcal{W}^{\pm}. \tag{16}$$

Now to evaluate the Evans function, it is only necessary to solve the two equations (16). As an example, take $n = 2$ and $B = I$, implying $n^{+} = 2 = n^{-}$. In the following calculation, the $\pm$ superscripts are suppressed since the same formula applies in both cases. In fact, we will adopt this as a standard notation—absence of the $\pm$ superscripts implies that the statement holds in both cases.

Lemma 2. *If $n = 2$ and $B = I$, then*

$$\mathcal{A}(x,\lambda) = \begin{pmatrix} 0 & 0 & 1 & -1 & 0 & 0 \\ -A_{12}' & A_{11} & A_{12} & 0 & 0 & 0 \\ \lambda - A_{22}' & A_{21} & A_{22} & 0 & 0 & 1 \\ A_{11}' - \lambda & 0 & 0 & A_{11} & A_{12} & -1 \\ A_{21}' & 0 & 0 & A_{21} & A_{22} & 0 \\ 0 & A_{21}' & \lambda - A_{11}' & A_{22}' - \lambda & -A_{12}' & A_{11} + A_{22} \end{pmatrix}. \tag{17}$$

Proof. Let

$$W_1 = \begin{pmatrix} x_1 \\ x_2 \\ x_3 \\ x_4 \end{pmatrix} \quad \text{and} \quad W_2 = \begin{pmatrix} y_1 \\ y_2 \\ y_3 \\ y_4 \end{pmatrix}.$$

Then using equations (8), (12) and (15),

$$\begin{aligned}
\mathcal{W}' &= (W_1 \wedge W_2)' = W_1' \wedge W_2 + W_1 \wedge W_2' \\
&= \tilde{A}W_1 \wedge W_2 + W_1 \wedge \tilde{A}W_2 = \tilde{A}W_1 \wedge W_2 - \tilde{A}W_2 \wedge W_1 \\
&= \sum_{i=1}^{4} \begin{pmatrix} \tilde{A}_{1i}x_i \\ \tilde{A}_{2i}x_i \\ \tilde{A}_{3i}x_i \\ \tilde{A}_{4i}x_i \end{pmatrix} \wedge W_2 - \sum_{j=1}^{4} \begin{pmatrix} \tilde{A}_{1j}y_j \\ \tilde{A}_{2j}y_j \\ \tilde{A}_{3j}y_j \\ \tilde{A}_{4j}y_j \end{pmatrix} \wedge W_1 \\
&= \sum_{i=1}^{4} \begin{pmatrix} \tilde{A}_{1i} \\ \tilde{A}_{2i} \\ \tilde{A}_{3i} \\ \tilde{A}_{4i} \end{pmatrix} \wedge (x_i W_2 - y_i W_1) = \sum_{i=1}^{4} \begin{pmatrix} \tilde{A}_{1i} \\ \tilde{A}_{2i} \\ \tilde{A}_{3i} \\ \tilde{A}_{4i} \end{pmatrix} \wedge \begin{pmatrix} x_i y_1 - x_1 y_i \\ x_i y_2 - x_2 y_i \\ x_i y_3 - x_3 y_i \\ x_i y_4 - x_4 y_i \end{pmatrix} \\
&= \mathcal{A}(W_1 \wedge W_2) = \mathcal{A}\mathcal{W}. \qquad \square
\end{aligned}$$

As before, "initial" conditions for (16) are supplied by Theorem 1, so it is necessary to have the eigenvalues and eigenvectors of $\mathcal{A}$. They are derived easily from the eigenvalues and eigenvectors of $\tilde{A}$, as the following lemma demonstrates.

Lemma 3. *Let $\mathcal{A}$ be defined as in equation* (16). *Then the eigenvalues and eigenvectors of $\mathcal{A}$ are $\mu_{i_1} + \cdots + \mu_{i_n}$ and $V_{i_1} \wedge \cdots \wedge V_{i_n}$ for $1 \le i_1 < \cdots < i_n \le m$, where μ_{i_j} and V_{i_j} are the eigenvalues and eigenvectors of the $2n \times 2n$ matrix $\tilde{A}$.*

Proof. Using relation (15),

$$\begin{aligned}
\mathcal{A}(V_{i_1} \wedge \cdots \wedge V_{i_n}) &= \sum_{j=1}^{n} V_{i_1} \wedge \cdots \wedge V_{i_{j-1}} \wedge \tilde{A}V_{i_j} \wedge V_{i_{j+1}} \wedge V_{i_n} \\
&= \sum_{j=1}^{n} V_{i_1} \wedge \cdots \wedge V_{i_{j-1}} \wedge \mu_{i_j} V_{i_j} \wedge V_{i_{j+1}} \wedge V_{i_n} \\
&= \left(\sum_{j=1}^{n} \mu_{i_j} \right) V_{i_1} \wedge \cdots \wedge V_{i_n}. \qquad \square
\end{aligned}$$

To emphasize the utility of the wedge product, recall that $W_1^-, \ldots, W_{n^-}^-$ are the only modes of W growing from $-\infty$. Therefore, Lemma 3 implies that $W_1^- \wedge \cdots \wedge W_{n^-}^-$ is *the fastest* growing mode of $\mathcal{W}$ from $-\infty$. Hence, it should be expected (and in fact is observed) that numerical approximation of this mode is accurate. The analogous argument from $+\infty$ also holds.

The second problem in calculating the winding number of $D[\Gamma]$ lies in partitioning Γ into subcontours Γ_i such that $D[\Gamma_i]$ lies in a slit plane; a slit plane being a subset of $\mathbb{C}$ of the form $\mathbb{C}\backslash\{r\alpha : 0 \neq \alpha \in \mathbb{C}, 0 \le r \in \mathbb{R}\}$. This will ensure that the calculated winding number is correct. But this is a difficult criterion to check. It is easier to partition Γ so that $D[\Gamma_i]$ is contained in a half plane whose boundary passes through the origin.

For $w, z \in \mathbb{C}$, define $\langle w, z \rangle$ to be the dot product between the real 2-vectors $(\mathrm{Re}(w), \mathrm{Im}(w))$ and $(\mathrm{Re}(z), \mathrm{Im}(z))$:

$$\langle w, z \rangle \doteq \mathrm{Re}(w)\mathrm{Re}(z) + \mathrm{Im}(w)\mathrm{Im}(z). \tag{18}$$

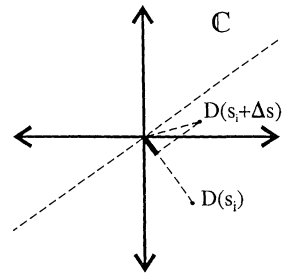

FIGURE 3. The projection of $D(s_i + \Delta s)$ onto $D(s_i)$.

Let a prime denote derivative with respect to s, the variable parametrizing Γ. Then if $\Gamma(s_i)$ is the starting point of Γ_i, it suffices to find s_{i+1} and $\beta \in [0, 1)$ such that

$$\langle D(s_i + \Delta s), \hat{D}(s_i)\rangle > \beta |D(s_i)| \tag{19}$$

for $0 \leq \Delta s \leq s_{i+1} - s_i$; here $\hat{D} = D/|D|$. In other words, the component of $D(s_i + \Delta s)$ in the direction of $D(s_i)$ should be a positive multiple of $D(s_i)$ (see Figure 3). Strictly speaking, the right side of inequality (19) could simply be 0. However, for quick stability determination, exact values for D will not be given at any point, and therefore some leeway is called for (and given by $\beta|D(s_i)|$). This condition allows us to check whether a given partition is appropriate. But a more useful condition gives s_{i+1} based on information at s_i, and thus forms the partition.

After expanding $D(s_i + \Delta s)$ in a Taylor series, condition (19) becomes, to second order,

$$|D(s_i)| + \Delta s\langle D'(s_i), \hat{D}(s_i)\rangle + (\Delta s)^2\langle D''(s_i), \hat{D}(s_i)\rangle/2 > \beta|D(s_i)|.$$

Thus, Δs is given by solutions of the following quadratic inequality at s_i:

$$(1/2)\langle D'', \hat{D}\rangle(\Delta s)^2 + \langle D', \hat{D}\rangle\Delta s + (1 - \beta)|D| > 0.$$

Notice that $\Delta s = 0$ always satisfies this condition (since $D \neq 0$ on Γ), so there will always be a positive value of Δs to choose. It is natural to try the value that satisfies

$$(1/2)\langle D'', \hat{D}\rangle(\Delta s)^2 + \langle D', \hat{D}\rangle\Delta s + (1 - \beta)|D| = 0.$$

But if $\langle D'', \hat{D}\rangle > 0$, there may be no solution or two negative solutions. In each case, the condition allows us to pick any positive value for Δs. Clearly, this is not useful. So, we force the sign of the second order term by noting that $\langle D'', \hat{D}\rangle > -|D''|$. This leaves us with the generally more conservative condition that Δs satisfy

$$-(1/2)|D''|(\Delta s)^2 + \langle D', \hat{D}\rangle\Delta s + (1 - \beta)|D| = 0, \tag{20}$$

or solving for Δs,

$$\Delta s = \frac{\langle D', \hat{D}\rangle + \sqrt{\langle D, \hat{D}\rangle^2 + 2(1 - \beta)|D''| \cdot |D|}}{|D''|}. \tag{21}$$

Note that Δs is well defined since the value given by equation (21) is always real and the other possible value is negative.

Using forward differences to approximate the derivatives of equation (21) leads to an algorithm suitable for quick (and apparently quite accurate) determination

of stability, typically on the order of 2 minutes per wave on a Pentium based PC. Also, in practice, β can usually be 0. However, in case of poor results, a positive value of β should be chosen as this will lead to smaller values for Δs.

3.4. **Error estimates.** Since the computation of D involves the numerical solution of an ODE, we must determine how accurate the computed values are. The analysis of a particular computation will reveal the sensitivity of the issue. For cubic model viscous shock 2 (see Figure 4, located in Section 4), and $\lambda = -0.00351563$,

$$\mathcal{W}^+(0) \approx (0.763, -0.187, -0.341, 0.0959, 0.187, -0.00291), \text{ and}$$
$$\mathcal{W}^-(0) \approx (0.0829, -0.0212, -0.0431, 0.0116, 0.0227, 0.000219).$$

The max norms of $\mathcal{W}^+(0)$ and $\mathcal{W}^-(0)$ are approximately 1 and 0.1, respectively. However,

$$D(\lambda) = \mathcal{W}^+(0) \wedge \mathcal{W}^-(0) \approx 4.7(10)^{-5},$$

so in calculating D by wedging the two 2-forms, numbers of nearly equal magnitude must be subtracted. As a crude approximation, two numbers of magnitude 1 are being subtracted with a result of magnitude 10^{-4}. So it can be expected that 3 or 4 significant digits are lost in this calculation of D. Since the relative error in D must be less than 1, the relative error in $\mathcal{W}^{\pm}(0)$ must be no larger than 10^{-4}. This is the required global relative error for a Runge-Kutta integration over a domain that may exceed length 100. But this is only an issue for points along the semicircular portion of Γ. The magnitude of D for other points along the contour is comparable to the max norms of $\mathcal{W}^+(0)$ and $\mathcal{W}^-(0)$.

Standard a priori error estimates will not yield such stringent bounds. Instead, the linearity of both equation (16) and the Runge-Kutta method will be exploited. Starting with some standard analysis, for a one step numerical scheme of the form $w_{n+1} = w_n + h_n\Psi(w_n, x_n, h_n)$ solving the equation $w' = f(x, w)$, derivation of global error bounds leads to the recursion

$$e_{n+1} = e_n + h_n\tau_n + h_n[\Psi(w_n, x_n, h_n) - \Psi(w(x_n), x_n, h_n)].$$

Here h_n is step size, e_n is the difference between the actual solution and approximate solution, and τ_n is a local truncation error. Taking norms on both sides and approximating $\Psi(w_n, x_n, h_n) - \Psi(w(x_n), x_n, h_n)$ with the help of the Lipschitz constant $\tilde{L}$,

$$|e_{n+1}| \le (1 + |h_n|\tilde{L})|e_n| + |h_n\tau_n|. \tag{22}$$

This gives an upper bound on the growth of $|e_n|$ from one step to the next.

Specializing to the case of an explicit Runge-Kutta scheme and $f(x, w) = A(x)w$ yields a much more useful error estimate. A general explicit Runge-Kutta scheme can be written

$$w_{n+1} = w_n + \sum_{i=1}^{m} c_i k_i, \tag{23}$$

where

$$k_1 = h_n f(x_n, w_n),$$
$$k_i = h_n f(x_n + a_i h_n, w_n + b_i k_{n-1}), \quad i = 2, 3, \ldots, m,$$

and the a_i, b_i, c_i, m are constants depending on the particular method [3]. Defining

$$A_1 = A(x_n),$$
$$A_i = A(x_n + a_i h_n)(I + b_i A_{i-1}), \quad i = 2, 3, \ldots, m,$$

the scheme becomes

$$\begin{aligned} w_{n+1} &= w_n + c_1 h_n A(x_n) w_n + \sum_{i=2}^{m} c_i h_n A(x_n + a_i h_n)(w_n + b_i k_{n-1}) \\ &= w_n + c_1 h_n A_1 w_n + \sum_{i=2}^{m} c_i h_n A(x_n + a_i h_n)(I + b_i A_{n-1}) w_n \\ &= w_n + h_n \left[\sum_{i=1}^{m} c_i A_i \right] w_n \\ &= [I + h_n M(x_n, h_n)] w_n, \end{aligned}$$

where $M(x_n, h_n) = \sum_{i=1}^{m} c_i A_i$. Hence $\Psi(w_n, x_n, h_n) = M(x_n, h_n) w_n$, and $e_{n+1} = e_n + h_n \tau_n + h_n M(x_n, h_n)(w_n - w(x_n))$, which simplifies to

$$e_{n+1} = [I + h_n M(x_n, h_n)] e_n + h_n \tau_n. \tag{24}$$

So, in this case, an *exact* error recursion results. But this recursion is not directly useful since only the magnitudes of e_0 and τ_n are known in practice.

A useful, rigorous error equation comes from solving the exact error recursion explicitly:

$$\begin{aligned} e_N &= P(N, 0) e_0 + \sum_{i=1}^{N-1} h_i P(N, i) \tau_i, \\ P(N, i) &= \prod_{j=i}^{N} [I + h_j M(x_j, h_j)]. \end{aligned} \tag{25}$$

Take norms on both sides to get the bound

$$|e_N| \le |P(N, 0)| \cdot |e_0| + \sum_{i=1}^{N-1} |h_i P(N, i)| \cdot |\tau_i|. \tag{26}$$

Estimate (26) is generally much sharper than estimate (22) since the essential difference is that between the norm of a product and the product of norms.

4. Applications

4.1. **A contrived system.** The eigenvalue equation

$$w''(x) = \frac{d}{dx} \left[\frac{\tanh(x/2)}{\sqrt{2}} \begin{pmatrix} -1 & -1 \\ -1 & 1 \end{pmatrix} w(x) \right] + \lambda w(x) \tag{27}$$

is a system whose associated Evans function can be computed analytically [2]. It is

$$D(\lambda) = 4C^2 \det \begin{pmatrix} -\kappa & 1-\sqrt{2} & \kappa & 1-\sqrt{2} \\ 1-\sqrt{2} & 1 & (\sqrt{2}-1)\kappa & 1 \\ \lambda & (\sqrt{2}-1)\kappa & \lambda & (1-\sqrt{2})\kappa \\ (\sqrt{2}-1)\lambda & -\kappa & (\sqrt{2}-1)\lambda & \kappa \end{pmatrix},$$

where $\kappa = \sqrt{\lambda + 1/4}$ and $C = 1/(1+2\kappa)$. A comparison of this analytic solution to the numerical solution using a fourth order adaptive Runge-Kutta scheme appears

TABLE 4.1. Comparison of estimated errors (26) and actual errors in computing the Evans function for a contrived system.

λ	Estimated Relative Error	Actual Relative Error
$2.25 - 9i$	0.0022571	$2.54(10)^{-6}$
$2.25 - 0.152189i$	0.0006853	$1.43(10)^{-6}$
$0 + 0.225i$	0.0016125	$6.07(10)^{-6}$
$-0.224943 + 0.0050524i$	3.67766	$6.75(10)^{-5}$

in Table 4.1. Note that estimated errors dwarf actual errors, but that estimated errors are still generally well below 1.

4.2. **The cubic model.** The cubic model

$$u_t + (|u|^2 u)_x = u_{xx}, \qquad u \in \mathbb{R}^2, \tag{28}$$

is an idealization of a system of equations relevant to magnetohydrodynamics [9]. It was shown by Liu and Freistuhler [9, 16, 15] that some of the viscous shock waves for the cubic model are stable. However, the method of proof only allows for showing that nearly linear profiles are stable.

TABLE 4.2. $\tilde{D}(-0.9/256)$ for the cubic model using a fourth order adaptive Runge-Kutta method.

τ	$\tilde{D}(-0.9/256)$	Estimated Relative Error	"Actual" Relative Error
10^{-5}	$3.63842(10)^{-5}$	49.7879	0.004209
10^{-6}	$3.64980(10)^{-5}$	5.66251	0.001095
10^{-7}	$3.65323(10)^{-5}$	0.640160	0.000156
10^{-8}	$3.65374(10)^{-5}$	0.0721777	0.000016
$\vdots$	$\vdots$		
0	$3.65380(10)^{-5}$		

TABLE 4.3. $\tilde{D}(1.12891 - 4.51562i)$ for the cubic model using a fourth order adaptive Runge-Kutta method.

τ	$\tilde{D}(1.12891 - 4.51562i)$	Estimated Relative Error	"Actual" Relative Error
10^{-4}	$-0.0202970 - 1.74920i$	89.4701	0.0004157
10^{-5}	$-0.0201544 - 1.74984i$	0.0453998	0.0000410
10^{-6}	$-0.0201400 - 1.74990i$	0.0008032	0.0000058
10^{-7}	$-0.0201385 - 1.74991i$	0.0000831	0.0000001
$\vdots$	$\vdots$		
0	$-0.0201383 - 1.74991i$		

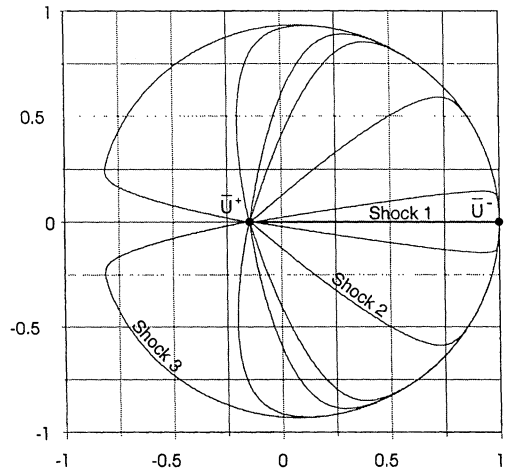

FIGURE 4. The family of viscous shock waves for the cubic model with $s = 7/8$ and $\overline{u}_- = (1, 0)$ fills a nearly circular region of the $\overline{u}_1$-$\overline{u}_2$ plane.

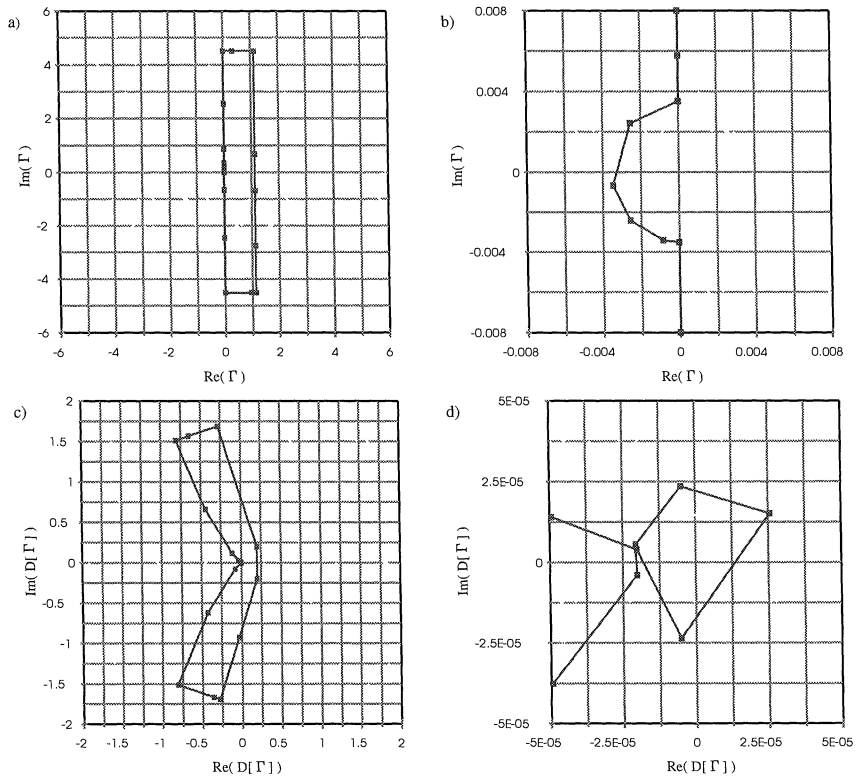

FIGURE 5. Γ in panels a) and b), and $D[\Gamma]$ in panels c) and d) for cubic model viscous shock 1.

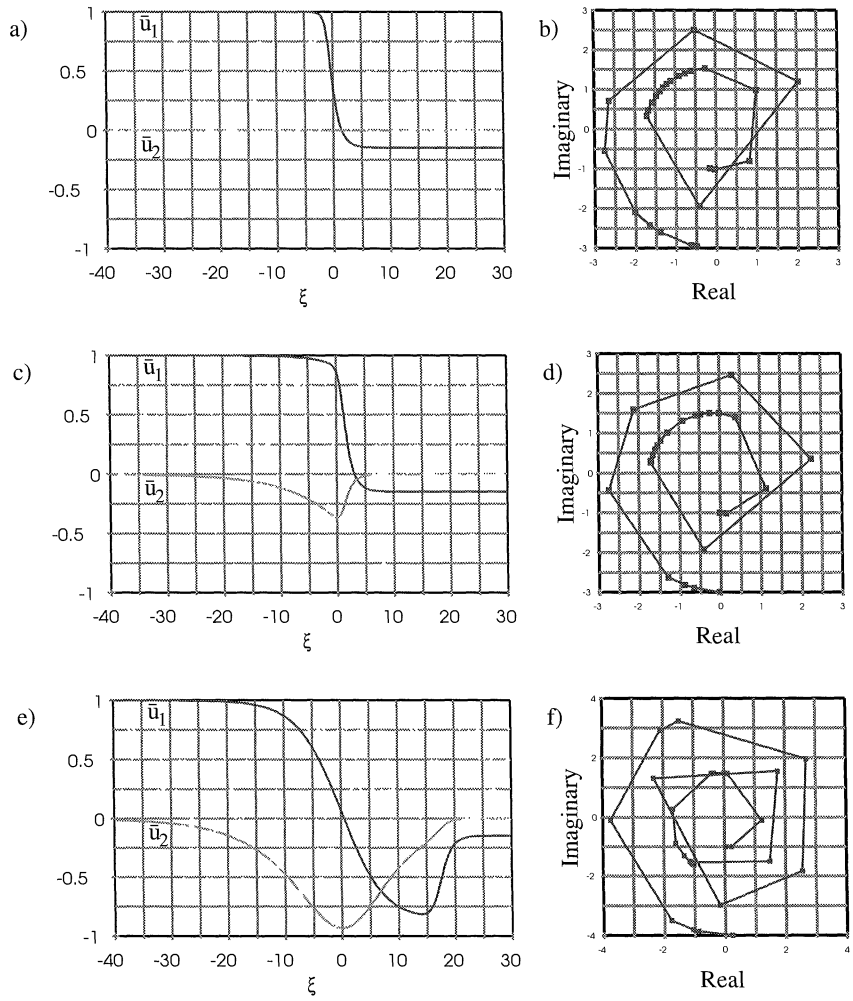

FIGURE 6. u vs. ξ in panels a), c) and e), and corresponding normalized Evans function (winding) plots in panels b), d) and f) for cubic model viscous shocks 1, 2 and 3.

Unlike the contrived system, there is no analytic solution of ODE (6) for the cubic model. We have to rely entirely on numerical estimates to gauge the accuracy of the Evans function method. In Tables 4.2 and 4.3, third order polynomial extrapolation was used to compute the values for $\tau = 0$. Other values of λ along Γ yield similar results. The underlying viscous shock wave is shock 2 of Figure 4.

The extrapolated values are used as exact values in computing "actual" relative errors. Notice that the estimated errors, computed using equation (26), are for the most part 1000 or more times the actual errors. So even these relatively sharp estimates are conservative. Also notice that $\tau = 10^{-5}$ is sufficient for calculating $D(1.12891 - 4.51562i)$ with approximate estimated accuracy 0.05 where $\tau = 10^{-8}$ is needed for calculating $D(-0.9/256)$ to roughly the same estimated accuracy. Here is numerical evidence of the loss of significance alluded to in subsection 3.4.

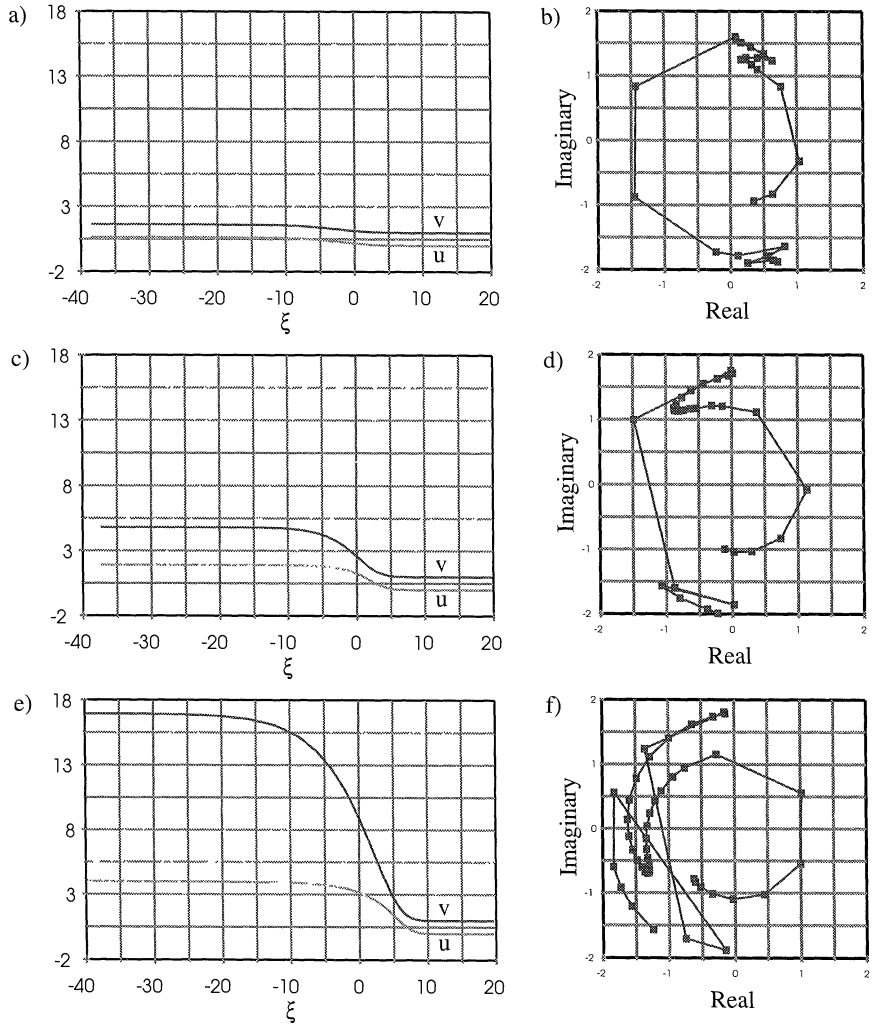

FIGURE 7. Viscous shock solutions of equation (30) with corresponding winding plots.

4.3. **Gas dynamics.** As for stability results, Figure 5, panels a) and c), show Γ and $D[\Gamma]$, respectively, for viscous shock 1 of Figure 4, but the winding number is not obvious. Panel c) shows the general shape of $D[\Gamma]$, but is unclear as to the winding since it looks as if the image passes through the origin. A closeup of the origin, panel d), shows that the image winds around the origin. But even this is unsatisfying, so $D[\Gamma]$ is normalized by the mapping

$$D \longmapsto (\arg D - \arg D_0)\frac{D}{|D|} \tag{29}$$

in Figure 6 panel b). Here it is clear that $D[\Gamma]$ winds twice around the origin for shock 1. Since the dimension of the stationary manifold for the cubic model is 2 (see Figure 4), this viscous shock wave is stable. Also, $D[\Gamma]$ (normalized by mapping (29)) winds twice and thrice around the origin for viscous shocks 2 and

3, respectively, (see Figure 6 panels d) and f)). So shock 2 is stable, but a little more investigation is needed for shock 3. A root search locates the eigenvalue on the negative real axis between -0.0015 and -0.0012, so shock 3 is also stable. Viscous shock 1 is nearly linear, so in this case we have simply verified numerically the analytic result of Freistuhler and Liu [9]. However, viscous shock 3 is strongly nonlinear, and so this stability result is new.

The equations of isentropic gas dynamics, or p-system, with artificial viscosity $B = I$ are

$$\begin{aligned} v_t - u_x &= v_{xx}, \\ u_t + P(v)_x &= u_{xx}. \end{aligned} \tag{30}$$

Three viscous shocks and their corresponding winding plots for $P(v) = v^{-2}$ are shown in Figure 7. All three shocks are stable since the dimension of M in this case is 1, which equals the number of times $D[\Gamma]$ revolves around the origin.

5. Discussion

The stability of contrived, strongly nonlinear (cubic model) and strong (gas dynamics) viscous shocks has been shown numerically. Beyond analyzing many more examples, the most immediate extension to this new capability is code that can handle nonidentity viscosity. In addition, efforts are being made to add the method to the Riemann Problem Package (RPP) [11] as an extension of its capability. This will allow the systematic exploration of viscous shock wave stability for families of conservation laws through an interactive graphical interface. In fact, the gas dynamics results of this paper have come from this effort while the others have come from [2].

Several improvements might be considered for the current algorithm in terms of speed or accuracy. For example, calculation of D' and D'' can be done directly giving more accurate values in equation (21), a higher order Runge-Kutta method could be used in the numerical integration for greater speed, or integrated equations [2] could be substituted to alleviate the problem of zeroes at the origin. But accuracy is already very good and would not likely improve significantly with implementation of these ideas. Furthermore, in practice it is computer science techniques, such as how to store data and the use of deflation, that prove more helpful in speeding up the calculation.

Finally, an interesting question is whether the present algorithm can be refined to the point of a numerical proof. While there are indications that this is a feasible project, using the ideas of [17] and [2] for example, it is still an open question.

Acknowledgments

Special thanks to the author's dissertation advisor, Kevin Zumbrun, for his invaluable guidance, insight, patience and attention to this work throughout the dissertation process and beyond. Also thanks to Dan Marchesin and Bradley Plohr who made the author's work on the the Riemann Problem Package possible. This work was partially supported by NSF grant INT-9216357, PCI/CNPq grant 171.446/97-6, and by IMPA, Rio de Janeiro, Brazil. Except where otherwise noted, this research was done at Indiana University during the author's tenure as a doctoral student. Portions of this paper appear in the author's dissertation.

References

[1] J. Alexander, R. Gardner, and C.K.R.T. Jones, *A topological invariant arising in the analysis of traveling waves*, J. Reine Angew. Math. **410** (1990), 167–212. MR **92d:**58028

[2] L.Q. Brin, *Numerical testing of the stability of viscous shock waves*, Ph.D. dissertation, Indiana University, May 1998.

[3] J.C. Butcher, *The numerical analysis of ordinary differential equations: Runge-Kutta and general linear methods*, John Wiley and Sons, New York, 1987. MR **88d:**65002

[4] W.A. Coppel, *Stability and asymptotic behavior of differential equations*, D. C. Heath and Company, Boston, Massachusetts, 1965. MR **32:**7875

[5] J.W. Evans, *Nerve axon equations. I. Linear approximations*, Indiana University Mathematics Journal **21** (1972), 877–885. MR **45:**1616

[6] ———, *Nerve axon equations: II. Stability at rest*, Indiana University Mathematics Journal **22** (1972), 75–90. MR **48:**1729

[7] ———, *Nerve axon equations. III. Stability of the nerve impulse*, Indiana University Mathematics Journal **22** (1972), 577–593. MR **52:**14697

[8] ———, *Nerve axon equations. IV. The stable and the unstable impulse*, Indiana University Mathematics Journal **24** (1975), 1169–1190. MR **52:**14698

[9] H. Freistuhler and T.-P. Liu, *Nonlinear stability of overcompressive shock waves in a rotationally invariant system of viscous conservation laws*, Communications in Mathematical Physics **153** (1993), 147–158. MR **94f:**35084

[10] R. Gardner and K. Zumbrun, *A geometric condition for stability of undercompressive viscous shock waves*, Preprint, 1997, to appear in CPAM.

[11] E. Isaacson, D. Marchesin, and B. Plohr, *Riemann problem package*, Unpublished software, available at `ftp://ftp.ams.sunysb.edu/pub/rp`.

[12] C.K.R.T. Jones, R. Gardner, and T. Kapitula, *Stability of traveling waves for nonconvex scalar viscous conservation laws*, Communications in Pure and Applied Math **46** (1993), no. 4, 505–526. MR **94c:**35123

[13] T. Kapitula and B. Sandstede, *Stability of bright solitary-wave solutions to perturbed nonlinear Schrödinger equations*, Phys. D **124** (1998) 58–103. MR **99h:**35199

[14] T. Kato, *Perturbation theory for linear operators*, Springer-Verlag, 1995. MR **96a:**47025

[15] T.-P. Liu, *Nonlinear stability of shock waves for viscous conservation laws*, Memoirs AMS **56** (1985), no. 328. MR **87a:**35127

[16] ———, *On the viscosity criterion for hyperbolic conservation laws, viscous profiles and numerical methods for shock waves*, SIAM (1991), 105–114. MR **92k:**35182

[17] D. Michelson, *Bunsen flames as steady solutions of the Kuramoto-Sivashinsky equation*, SIAM Journal of Mathematical Analysis **23** (1992), no. 2, 364–386. MR **92j:**35179

[18] ———, *Stability of the Bunsen flame profiles in the Kuramoto-Sivashinsky equation*, SIAM Journal of Mathematical Analysis **27** (1996), no. 3, 765–781. MR **97b:**80009

[19] D.M. Michelson and G.I. Sivashinsky, *Nonlinear analysis of hydrodynamic instability in laminar flames. II. Numerical experiments*, Acta Astronautica **4** (1977), 1207–1221. MR **58:**32374

[20] O. Oleinik, *Uniqueness and stability of the generalized solution of the Cauchy problem for a quasilinear equation*, Usp. Mat. Nauk. **14** (1959) 165–170; English translation in *Amer. Math. Soc. Transl. Ser. 2*, 1964, 285-290. MR **22:**8187

[21] B.P. Palka, *An introduction to complex function theory*, Springer-Verlag, 1991. MR **92b:**30001

[22] K. Zumbrun and P. Howard, *Pointwise semigroup methods and stability of viscous shock waves*, Indiana Univ. Math. J. **47** (1998) 741–871. MR **99m:**35137

Southern Connecticut State University, Department of Mathematics, New Haven, Connecticut 06515

E-mail address: `brin@southernct.edu`